applied mechanics

MDPI

Article

Experimental Investigation of the Seismic Response of Small Freestanding Replicas of Ancient Vessels

Angeliki Papalou

Civil Engineering Department, University of the Peloponnese, 26334 Patras, Greece; papalou@uop.gr

Abstract: Monumental artifacts belong to our cultural heritage, and there is a great need to protect them from earthquake damage. This study experimentally investigates the behavior of replicas of ancient vessels under seismic excitations. Each vessel was placed on a wooden base, which was attached to a shake table and was excited by earthquake signals. The effect of the amplitude of the excitation and the friction coefficient between the object and the base of support was examined. The dynamic response of the vessels included sliding and rocking, which, at high excitation levels, could involve rotation about their vertical axis and translation motion. High levels of excitation could cause the vessels to overturn but this did not always occur at the same level of excitation. The coefficient of friction is a key parameter of their behavior. If it is high, sliding motion is reduced while rocking parallel to the direction of excitation increases, starting at low excitation levels. This could lead to an early overturning of the object. The geometric characteristics and irregularities of the vessel can play an important role in its dynamic response.

Keywords: ancient vessels; seismic excitation; monumental objects; artifacts

Citation: Papalou, A. Experimental Investigation of the Seismic Response of Small Freestanding Replicas of Ancient Vessels. *Appl. Mech.* **2024**, *5*, 856–876. https://doi.org/10.3390/applmech5040048

Received: 21 August 2024
Revised: 16 October 2024
Accepted: 18 November 2024
Published: 20 November 2024

1. Introduction

The preservation of monumental objects (artifacts) is of great importance. Vibrations can create significant damage to artifacts. Several museums have reported damage to their artifacts after earthquakes. For example, in 1999, a strong earthquake in Athens damaged artifacts in the National Museum [1,2]. In 2016, statues collapsed due to earthquakes in Italy [3]. In Zagreb (2020) and Turkey (2023), historical buildings and museum objects suffered from damage after strong earthquakes.

Artifacts placed in museums can be damaged if other objects fall on them or if they start moving due to the vibration of their base of support. Several studies have investigated the vulnerability of museums' objects due to earthquakes and examined techniques to mitigate their damage [3–9].

Past analytical and numerical studies mainly examined the dynamic behavior of rigid objects of rectangular shape and their conditions of sliding, rocking, and overturning, focusing mostly on plane motion [10–20]. Numerical simulations extended the investigation of the dynamic behavior of art objects of different shapes [13,21].

Experimental studies have examined the dynamic behavior of rigid blocks with shake tables tests [22,23], the seismic assessment of a tall ceramic vase [24], the dynamic behavior of typical museum arrangements [25], and the dynamic behavior and vibration protection of ancient columns and statues [26,27].

The study of the dynamic behavior of artifacts with different sizes and materials can give more information about their behavior under strong earthquakes and can lead to improved protection measures. Past studies have shown that the dynamic behavior of art objects includes mostly sliding and rocking if certain conditions are satisfied [1,11]. Rocking can lead to overturning, which can damage the object. Sliding can be acceptable if it is limited; otherwise, collisions may occur with other objects or the walls of their display

case. In addition, if the objects are fixed to their base, internal stresses that will develop due to vibration may exceed their strength.

Most of the studies examined the behavior of freestanding objects numerically, considering them as rigid bodies responding to the seismic excitation by sliding and rocking, neglecting rotation about vertical axes. In addition, the criteria for rocking or sliding and the effect of the coefficient of friction on their behavior have been mostly identified by considering regular rectangular objects [28]. Limited experimental studies have examined the dynamic behavior of objects with irregular geometry [24].

This study experimentally examines the dynamic behavior of replicas of freestanding small ancient vessels under earthquake excitations. Small vessels with different geometric characteristics were placed on a wooden base that was attached to a shake table. Their dynamic response was measured. The influence of the coefficient of friction and the intensity of excitation were investigated. The criteria of rocking, sliding, and overturning were also examined. The findings of this research are not limited to ancient vessels but can be extended to any artifacts of similar shape.

2. Experimental Investigation

Small freestanding replicas of ancient vessels with different geometric characteristics were used. These included two red-figured lekythos, one amphora, and one crater (Figure 1). The geometric characteristics of the vessels are presented in Table 1, where b corresponds to half the diameter of the bottom of the vessel and h the distance of the center of gravity of the vessel from its plane of support.

Figure 1. Photograph of the vessels that were used in the experiments.

Table 1. Geometric characteristics of the vessels used in the experiments.

No.	Description	Mass (gr)	Height (cm)	Bottom Diameter (cm)	Top Diameter (cm)	b/h
1	Large Lekythos	420	24	5.7	4.8	0.26
2	Small Lekythos	175	16	4.5	3.3	0.32
3	Amphora	1490	32	10	12.3	0.36
4	Krater	576	16.8	7.2	15.6	0.52

The laboratory tests were conducted by setting each vessel on a wooden base (melamine support base) that was fixed on a shake table by using steel angles. A safety frame was placed around the experimental set-up. Loose strings connected the top part of the safety frame with the vessels' handles to prevent them from falling. The shake table applied the excitation horizontally in one direction.

Two sets of experiments were performed for each vessel. In the first set, the coefficient of friction between the plane of support and the object was approximately $\mu = 0.28$ (small coefficient of friction) for all objects. In the second set, a layer of felt was added, increasing the coefficient of friction to $\mu = 0.41$ (large coefficient of friction). Determining the coefficient of friction for the vessels was challenging due to their geometry. When placed on an incline in the upright position, they would overturn before sliding, making it difficult to obtain the angle at which sliding would occur. For that reason, the coefficient of friction was determined by placing the vessels (as well as a flat ceramic object) lying down on the surfaces of contact and measuring the tangent of the angle that would invoke sliding. According to physics, the coefficient of friction is equal to the tangent of the angle at which the object is about to slide.

The displacement and acceleration of the support base were measured with a draw wire (Waycon, 225 mm) and an accelerometer (Kistler, ± 2 g), respectively. Initially, the dynamic behavior of the vessels was observed for all earthquake signals used, measuring only the motion of the base. Later on, the motion of the vessels was recorded. This was challenging due to their small mass and curved geometry. Three laser transducers (Waycon, LAS-T-500-A, Series 1,440,221, 100–600 mm, Taufkirchen, Germany) were used to measure the displacement of all vessels. The top acceleration was measured only for the amphora because it was the only vessel with substantial mass such that the addition of the accelerometer would not affect its motion. Two of the laser transducers measured the displacement of the top and lower part of the vessel parallel to the direction of the excitation. The third transducer measured the displacement of the top part of the object perpendicular to the direction of the excitation. An 8-channel sensor interface system (Kyowa PCD-330B-F, Tokyo, Japan) was used to collect the data from the sensors. Since the irregularity in geometry could affect the results during rocking, and the motion of the object could be large enough that it could not be captured from the transducers for all excitation levels, lightweight rectangular cardboards were attached at the top and lower part of the vessel (Figure 2). The use of cardboard provided a more accurate estimation of the vessel's response as long as the laser transducers maintained contact with the vessel, which was the case most of the time. In a few instances, when the rotation was significant and the instruments lost contact with the vessel, extremely high readings were produced, which were easily identifiable and were not considered peak displacements. Large rotation occurred only for a few of the cases examined for high levels of excitation. Even though significant rotation may reduce the accuracy of the results, a good estimation of the vessel's movement can still be obtained. Most of the experiments were recorded by a camera. Hand measurements were taken at the end of each experiment to identify if the vessel moved from its original position.

The excitation consisted of earthquake signals with different frequency spectrums. The intensity of the signals was increased gradually until the overturning of the vessel. In this article, the results from an earthquake, with a frequency spectrum in the range of 0–6 Hz, are presented. This earthquake (DOI: 10.5281/zenodo.12679347) was selected due to its broad frequency spectrum. Figure 3 depicts the time history and frequency spectrum of the earthquake signal for one of the levels of excitation used in the experiments. The acceleration and displacement were measured by the instruments, and the velocity was obtained from the acceleration by integration. Mathworks, MATLAB, Release 2022b was used, for the graphical representation of the data.

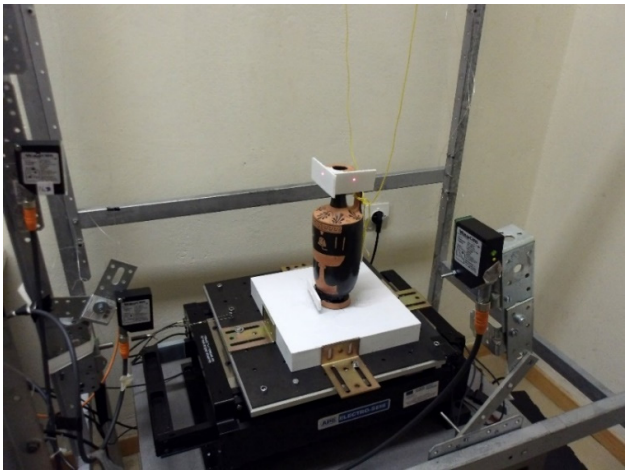

Figure 2. Photograph of the experimental set-up.

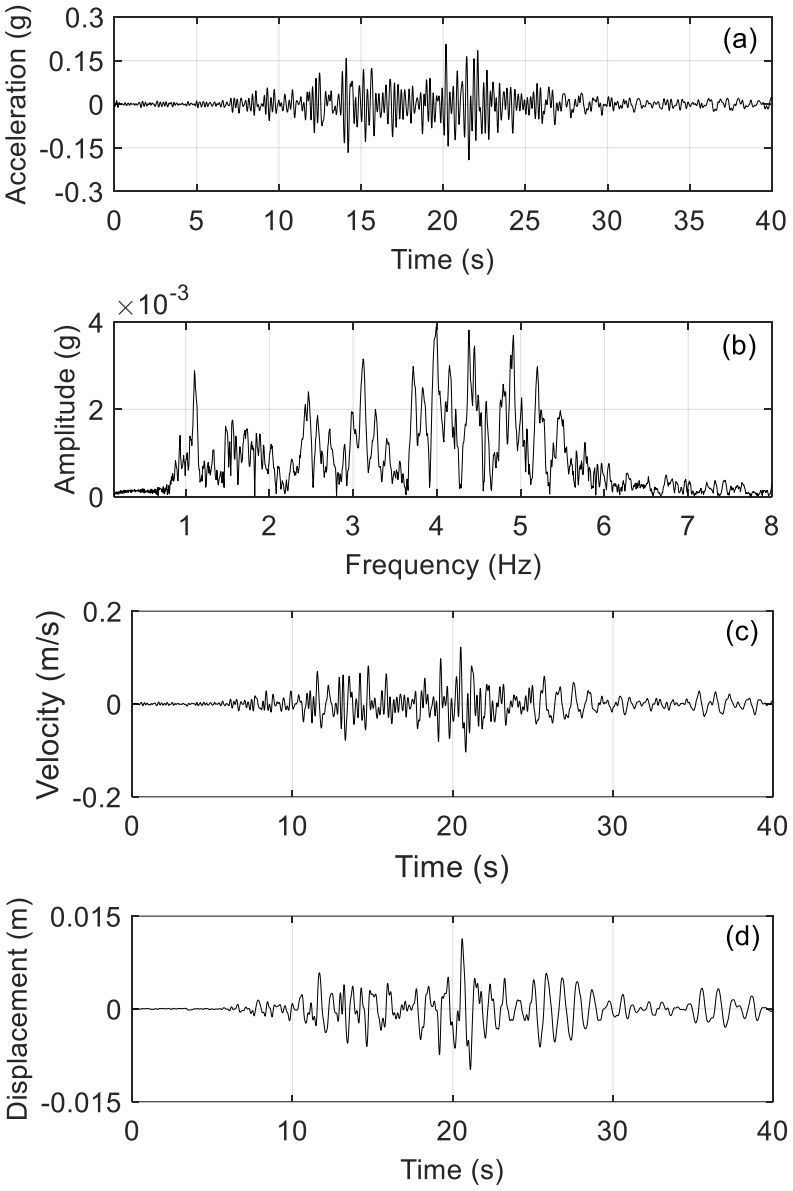

Figure 3. Base excitation: (**a**) acceleration; (**b**) its frequency spectrum; (**c**) velocity; and (**d**) displacement time history.

3. Experimental Results

The dynamic response of the vessels, depending on the surface of their base, included sliding, rotation, and rocking, which could lead to overturning. In the next sections, the dynamic response of the vessels examined in the experiments is described in detail.

3.1. Large Lekythos

Initially, the large lekythos was placed on the wooden base where the coefficient of friction between the plane of support and the object was approximately equal to 0.28 (small coefficient of friction). Figure 4 presents the peak relative displacement (relative to the base of support) of the top and lower part of the vessel with respect to the peak base acceleration. In addition, the peak displacement of the top part of the vessel perpendicular to the direction of the excitation is also presented. The logarithmic scale was selected to present the peak displacement due to the wide range of values. At lower levels of excitation, slight motion of the vessel's upper part was observed with no visible movement of its base. Visible rocking started when the peak acceleration was close to 0.18 g. At higher excitation levels, rotation around the vessel's vertical axis occurred simultaneously with rocking. This can be observed in Figure 5, which features images taken from a video that recorded the motion of the object when it was subjected to the earthquake excitation level that led to its overturning. The distance between the two curves corresponding to the maximum displacement of the top and bottom of the vessel indicates that rocking took place. At higher levels of excitation, the peak displacement of the top part of the vessel parallel and perpendicular to the direction of the excitation were approaching each other. Overturning occurred when the peak velocity and acceleration of the excitation were close to 0.14 m/s and 0.25 g, respectively. In other earthquake excitation signals, the object sometimes fell when the excitation level was high enough, while sometimes (at the same excitation level) it would rock and rotate, coming very close to falling, but, at the last instance, it would find its balance, avoiding a fall.

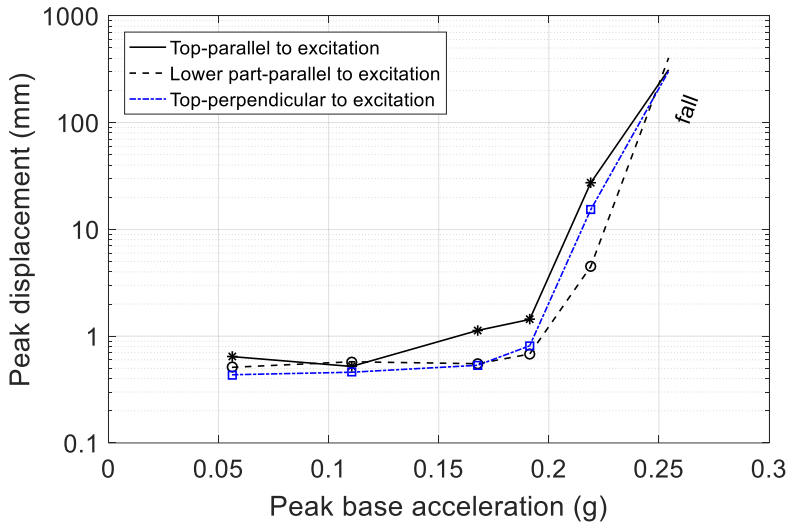

Figure 4. Peak displacement of the large lekythos under different intensity levels of the earthquake excitation (small coefficient of friction).

Figure 6 depicts the relative displacement of the large lekythos for a peak acceleration of 0.23 g, which is smaller but close to the peak acceleration that caused overturning. In the lower part of the Figure, the base acceleration was added to understand the behavior of the object with respect to the excitation. At low levels of excitation, the object's base remained stationary until the excitation reached a certain point. However, the top of the object might move slightly due to irregularities and imperfections in its base without visible lifting from the support surface. Rocking motion started after the 20th second of the excitation which can be observed by the difference that exists between the displacement of the top and

lower part of the vessel. According to theory, as mentioned in the following discussion section, several conditions must be satisfied for the object to start rocking or sliding. These conditions were not satisfied prior to the 20th second. Actually, rocking started a little earlier than predicted by the theory. Considerable motion also existed perpendicular to the direction of the excitation, including rotation of the object about its vertical axis. The object's final position was approximately 3 mm and 2 mm, far from its start position, parallel and perpendicular to the direction of excitation, respectively. This translation occurred as the object was rocking.

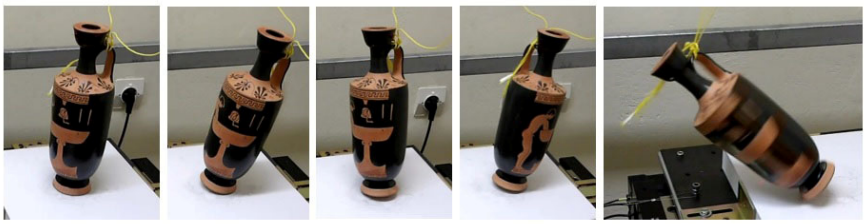

Figure 5. Photographs showing the seismic response of the large lekythos (small coefficient of friction). Rotation of the large lekythos about its vertical axis is observed.

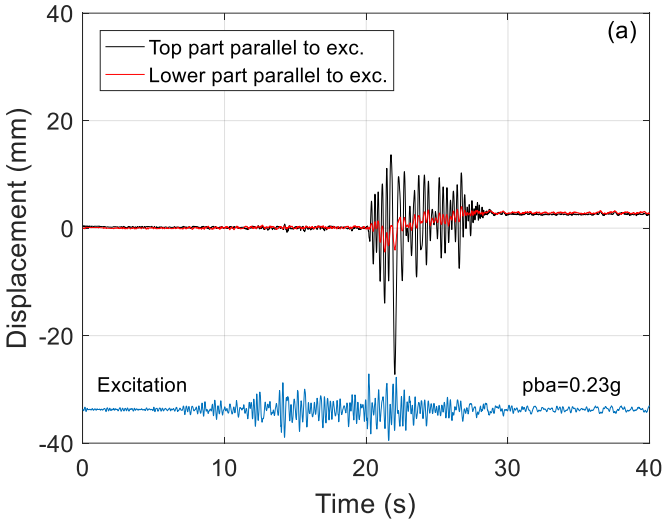

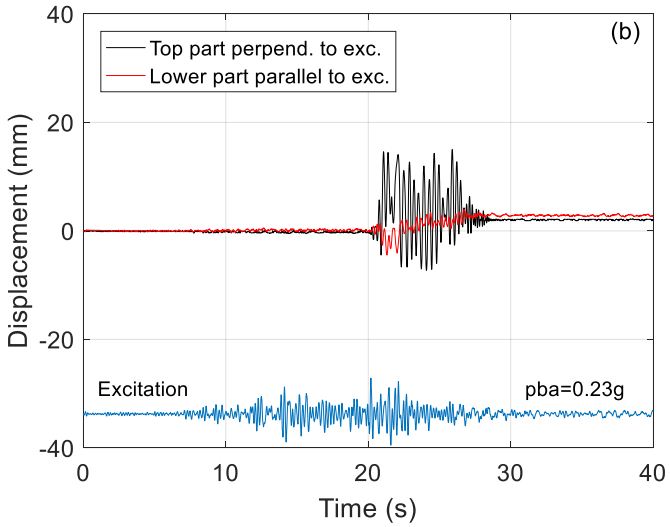

Figure 6. Response displacement of the large lekythos for peak base acceleration (pba) 0.23 g: (**a**) top and lower parts parallel to the direction of excitation; (**b**) lower part parallel and top part perpendicular to the direction of excitation (small coefficient of friction).

The seismic behavior of the vessel changed when the coefficient of friction increased (Figure 7). A slight motion of the vessel's top was observed even at the lowest excitation levels, with no visible lifting from its base. Visible rocking started when the peak base acceleration was close to 0.12 g, which is obvious from the distance between the two curves corresponding to the peak displacement of the top (solid black curve) and bottom parts (dashed black curve) of the vessel. The vessel moved mostly parallel to the direction of the excitation (Figure 8) without rotation. Overturning occurred when the peak velocity and peak acceleration of the excitation were close to 0.14 m/s and 0.25 g, respectively. The increase in the coefficient of friction reduced the motion perpendicular to the direction of excitation and the rotation about its vertical axis but did not alter the level of excitation at which overturning occurred.

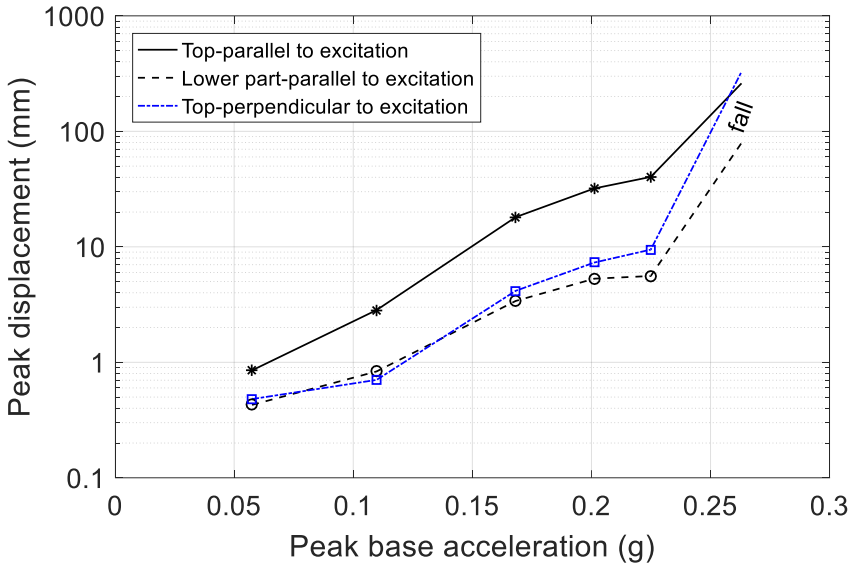

Figure 7. Peak displacement of the large lekythos under different intensity levels of the earthquake excitation (large coefficient of friction).

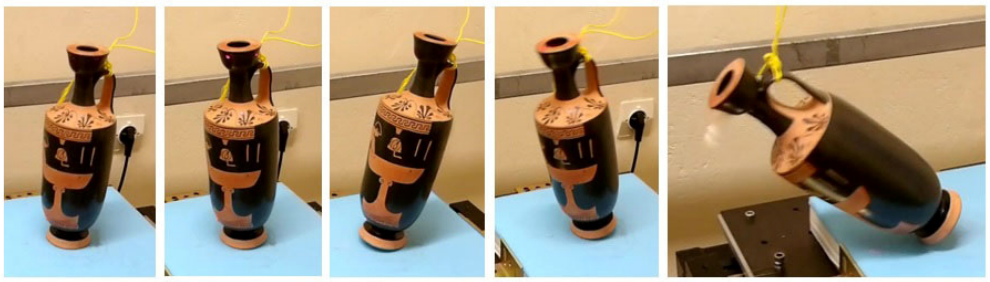

Figure 8. Photographs showing the seismic response of the large lekythos (large coefficient of friction). No rotation is observed.

Figure 9 depicts the relative displacement of the vessel for a peak acceleration of 0.22 g, which is a little smaller than the peak acceleration that caused the overturning. Rocking started early since there was a difference in amplitudes between the top and lower parts of the vessel. The object's final position was approximately 2 mm away from its starting position, parallel to the direction of excitation. This change in position occurred as the object was rocking. The motion of the top part of the object perpendicular to the direction of the excitation was small. Figures 6 and 9 show the response of the vessel at approximately the same level of excitation. The response was different due to the coefficient of friction. The increase in the coefficient of friction caused rocking to occur much earlier and reduced the motion perpendicular to the direction of excitation.

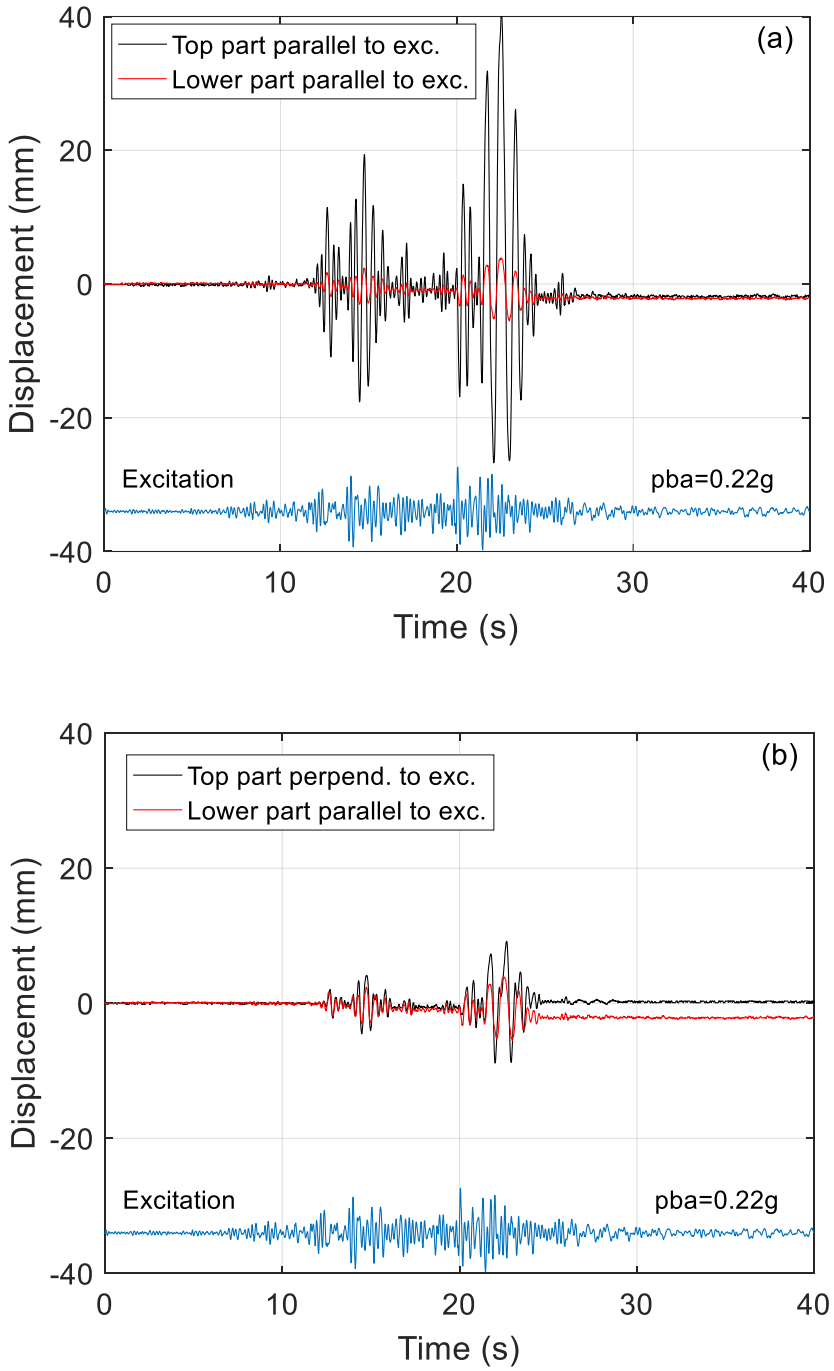

Figure 9. Response displacement of the large lekythos for peak base acceleration 0.22 g: (**a**) top and lower parts parallel to the direction of excitation; (**b**) lower part parallel and top part perpendicular to the direction of excitation (large coefficient of friction).

3.2. Small Lekythos

In the next set of experiments, the small lekythos was placed on the wooden base (small coefficient of friction). The main dynamic response of this vessel was sliding parallel to the direction of the excitation (Figure 10). This can be observed by the closeness of the two curves representing the motion of the top and lower parts of the vessel parallel to the direction of excitation. Sliding and rocking were observed at high excitation levels and close to the level that the object would fall (Figure 11). Overturning occurred when the peak velocity of the support base was close to 0.22 m/s. Higher excitation levels, compared to the large lekythos, were required for the object to fall.

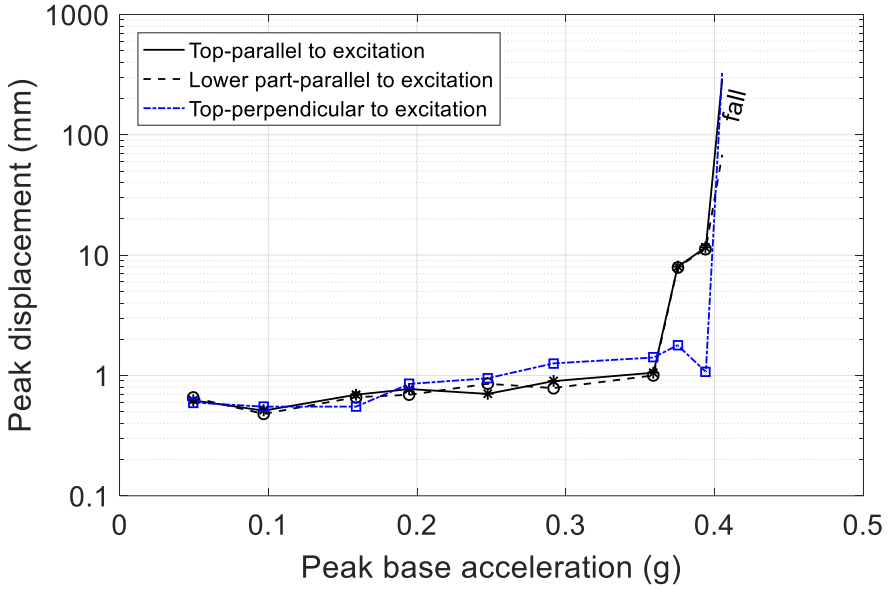

Figure 10. Peak displacement of the small lekythos under different intensity levels of the earthquake excitation (small coefficient of friction).

Figure 11. Photographs showing the seismic response of the small lekythos (small coefficient of friction).

Figure 12 depicts the displacement of the vessel for a peak acceleration of 0.36 g, which is slightly lower than the peak acceleration that caused overturning. It is observed that no rocking occurred since the motion of the top part and lower part coincided. Sliding began occurring after the 20th second when the excitation was strong enough to overcome the friction. The object was sliding back and forth parallel to the direction of the excitation till it reached its final position, which was approximately 7 mm away from its starting position. Sliding perpendicular to the direction of the excitation was very small.

The seismic behavior of the vessel was altered when the coefficient of friction increased (Figure 13). Sliding was minimized while visible rocking began at approximately 0.17 g. Overturning occurred when the peak velocity of the support base was close to 0.14 m/s. The influence of the surface on the dynamic behavior of the small lekythos was significant. The object overturned at almost half the base acceleration level required for low friction (Figure 10).

Figure 14 depicts the relative displacement of the vessel for a peak acceleration of 0.23 g, which is smaller but close to the peak acceleration caused by overturning. The difference in displacement between the top and lower parts of the vessel indicates that the rocking motion began around the 15th second of the excitation, corresponding to a base acceleration of 0.15 g. Weaker motion occurred perpendicular to the direction of excitation. The object's final position was approximately 1.5 mm far from its starting position, parallel and perpendicular to the direction of excitation. The increase in the coefficient of friction resulted in the motion of the vessel occurring much earlier, reduced sliding, and introduced intense rocking parallel to the direction of excitation.

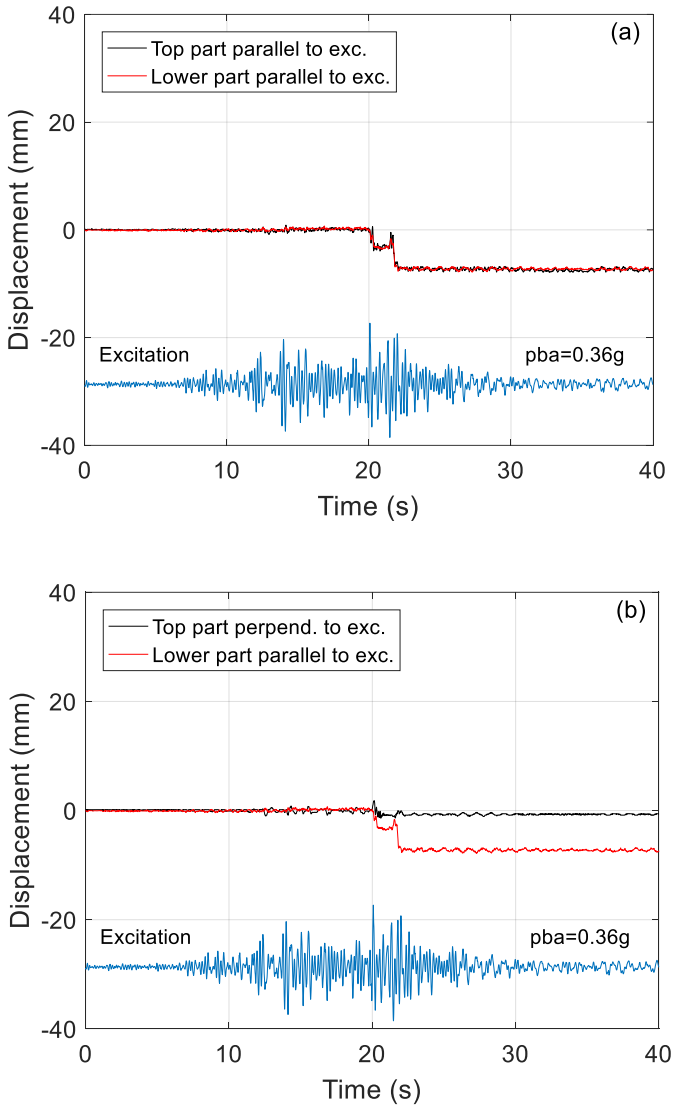

Figure 12. Response displacement of the small lekythos for peak base acceleration (pba) 0.36 g: (**a**) top and lower parts parallel to the direction of excitation; (**b**) lower part parallel and top part perpendicular to the direction of excitation (small coefficient of friction).

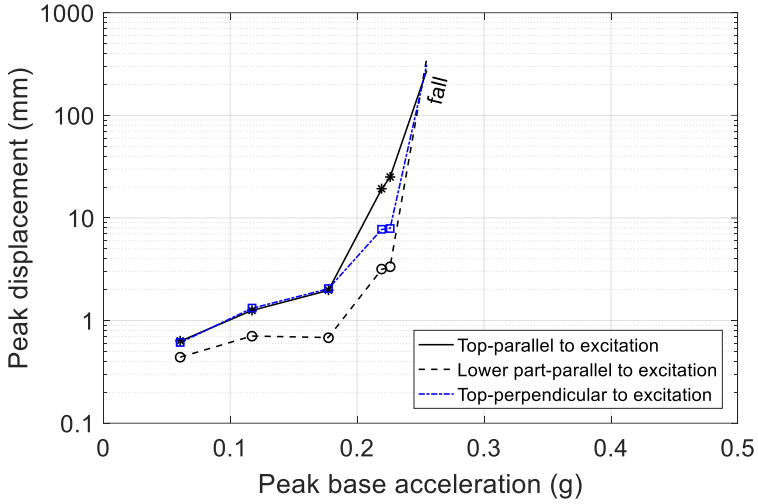

Figure 13. Peak displacement of the small lekythos under different intensity levels of the earthquake excitation (large coefficient of friction).

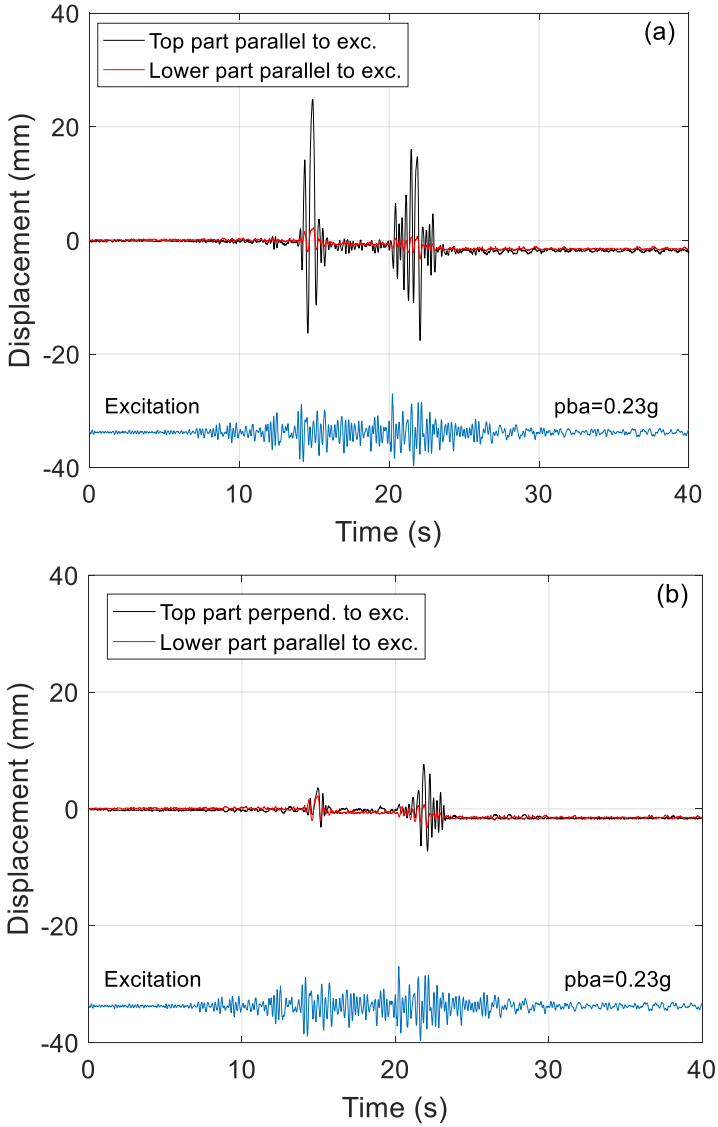

Figure 14. Response displacement of the small vessel for peak base acceleration (pba) 0.23 g: (**a**) top and lower parts parallel to the direction of excitation; (**b**) lower part parallel and top part perpendicular to the direction of excitation (large coefficient of friction).

3.3. Amphora

In the next set of experiments, the amphora was used. For the small coefficient of friction, rocking was the primary motion of the object, beginning at low levels of excitation. At higher levels of excitation, rocking intensified, and the amphora rotated about its vertical axis, reaching levels up to 90° (Figure 15). The object sometimes would fall when the excitation level was high enough, and sometimes, at the same excitation level, it would rock, rotate, and be very close to falling, but at the last instance, it would find its balance without falling. This is depicted in Figure 16, with the red dots presenting the point where there is a high possibility of overturning from the corresponding excitation level and above. The peak velocity of the base at this point was 0.23 m/s.

Figure 17 depicts the relative displacement of the vessel for a peak acceleration of 0.35 g. The motion included intense rocking with rotation and a final displacement of approximately 2 cm from its initial position, both parallel and perpendicular to the direction of excitation. Rocking started early when the peak base acceleration was close to 0.15 g.

Figure 15. Photographs showing the seismic response of the amphora (small coefficient of friction). Rotation of the amphora about its vertical axis is observed.

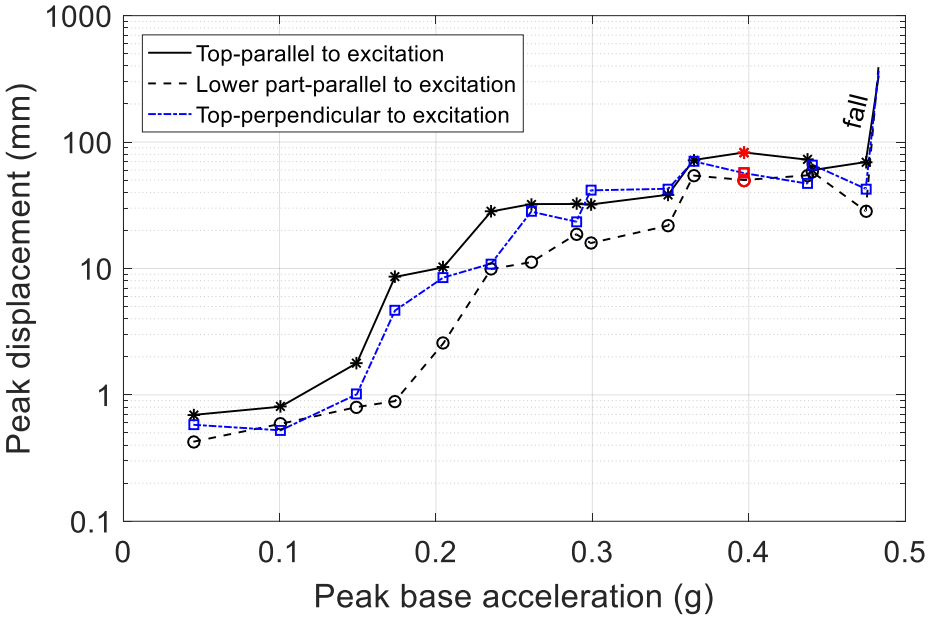

Figure 16. Peak displacement of the amphora under different intensity levels of the earthquake excitation (small coefficient of friction).

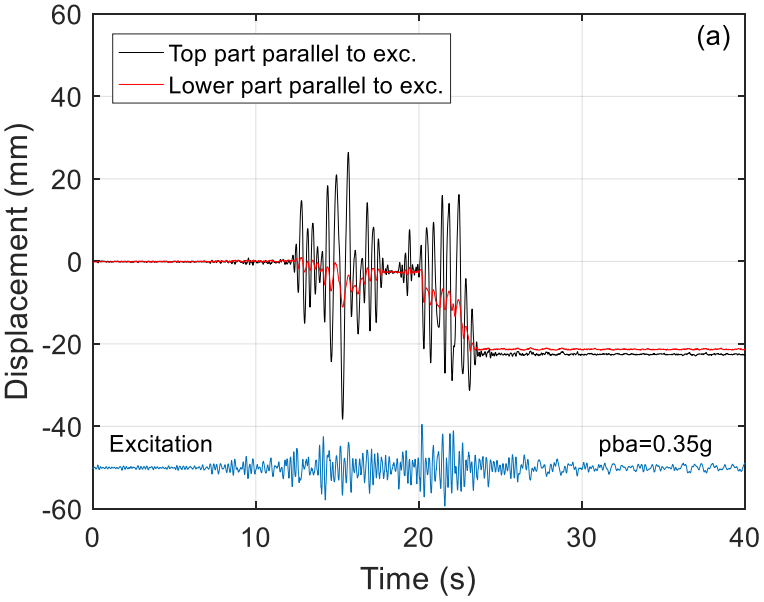

Figure 17. *Cont.*

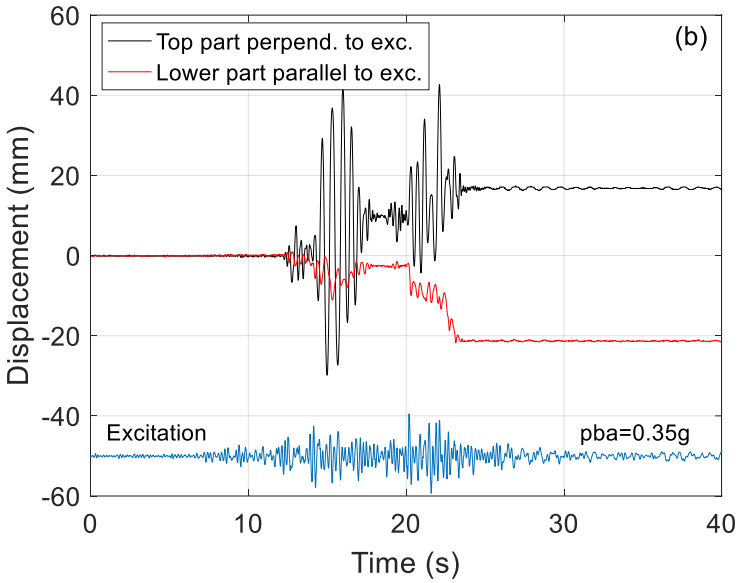

Figure 17. Response displacement of the amphora for peak base acceleration (pba) 0.35 g: (**a**) top and lower parts parallel to the direction of excitation; (**b**) lower part parallel and top part perpendicular to the direction of excitation (small coefficient of friction).

The increase in the coefficient of friction minimized the rotation of the amphora about its vertical axis (Figure 18). Its final position could be 1–2 cm away from its starting position. Overturning occurred when the peak velocity of the excitation was close to 0.25 m/s. Figure 19 presents the peak displacement with respect to the peak base acceleration. The difference between the peak displacement of the lower part and the top part of the vessel indicates that rocking started at low levels of excitation. The coefficient of friction played a less important role than in the previous cases examined.

Figure 18. Photographs showing the seismic response of the amphora (large coefficient of friction).

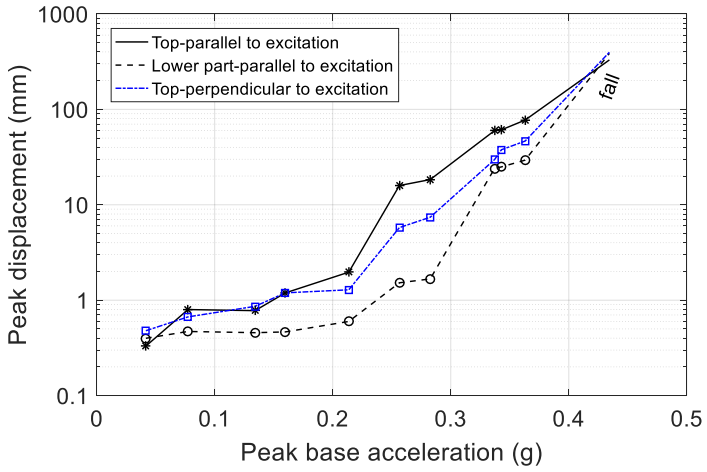

Figure 19. Peak displacement of the amphora under different intensity levels of the earthquake excitation (large coefficient of friction).

Figure 20 depicts the response displacement of the vessel for a peak acceleration of 0.37 g. The motion included intense rocking with small rotation and final displacement from its initial position by approximately 15 mm perpendicular to the direction of excitation. Rocking started early when the peak base acceleration was close to 0.15 g. The increase in friction increased rocking parallel to the direction of excitation but reduced the rotation of the object.

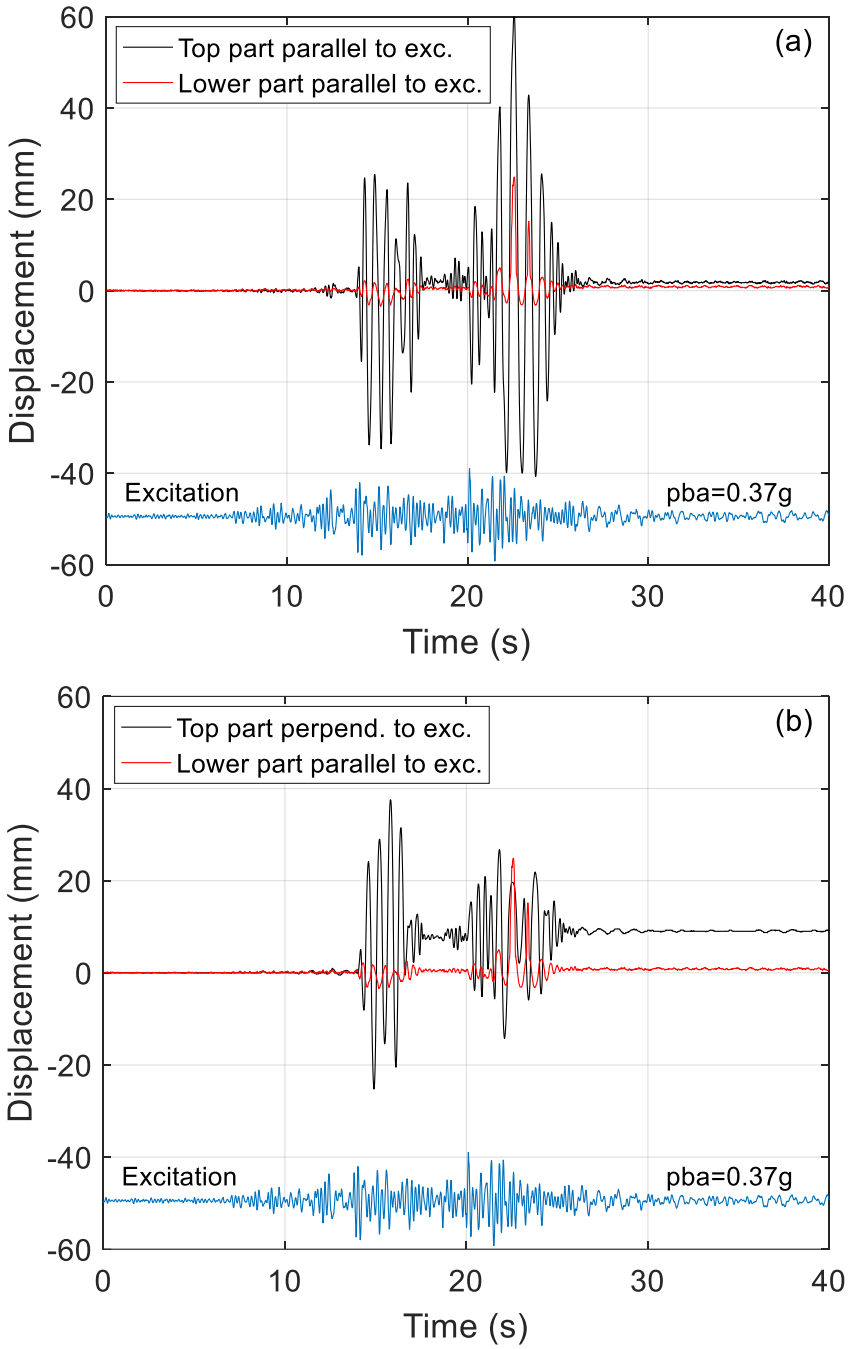

Figure 20. Response displacement of the amphora for peak base acceleration (pba) 0.37 g: (**a**) top and lower parts parallel to the direction of excitation; (**b**) lower part parallel and top part perpendicular to the direction of excitation (large coefficient of friction).

3.4. Krater

In the next set of experiments, the response of the krater was examined. High excitation levels (greater than 0.35 g) were needed for the krater to overcome friction. For the small

coefficient of friction, sliding occurred mostly in the direction parallel to the excitation. No rocking or rotation was observed (Figure 21), and the peak displacement of the top and lower parts of the object practically coincided. Increasing the level of excitation increased the sliding without rocking or overturning (up to a level of excitation with a peak velocity of 0.44 m/s). At the high levels of excitation, the vessel would slide back and forth.

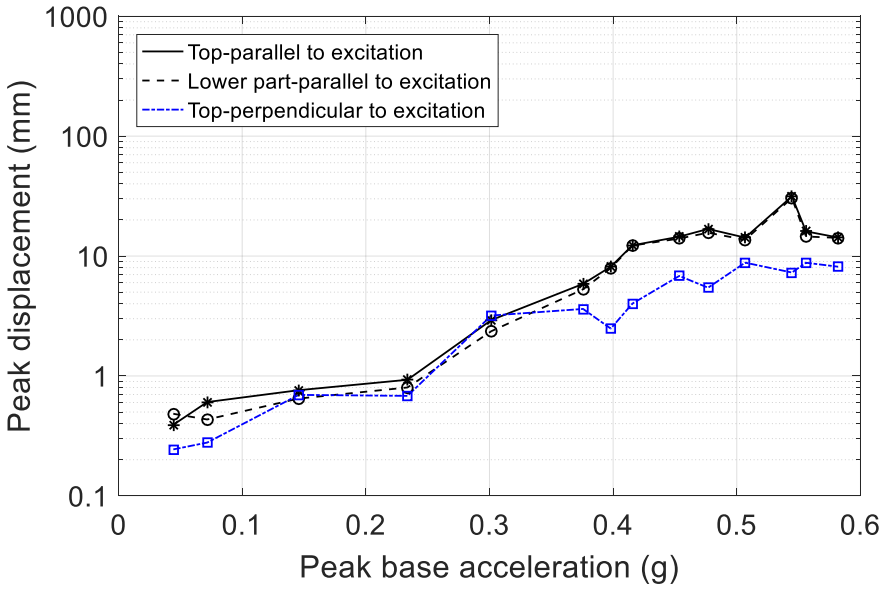

Figure 21. Peak displacement of the krater under different intensity levels of the earthquake excitation (small coefficient of friction).

Figure 22 depicts the response relative displacement of the vessel for a peak acceleration of 0.55 g. The motion of the object included sliding, starting at peak base acceleration close to 0.14 g. In addition, small sliding occurred perpendicular to the direction of excitation. The object's final position was approximately 13 mm and 7 mm far from its starting position, parallel and perpendicular to the direction of excitation, respectively. The object moved back and forth parallel to the direction of excitation.

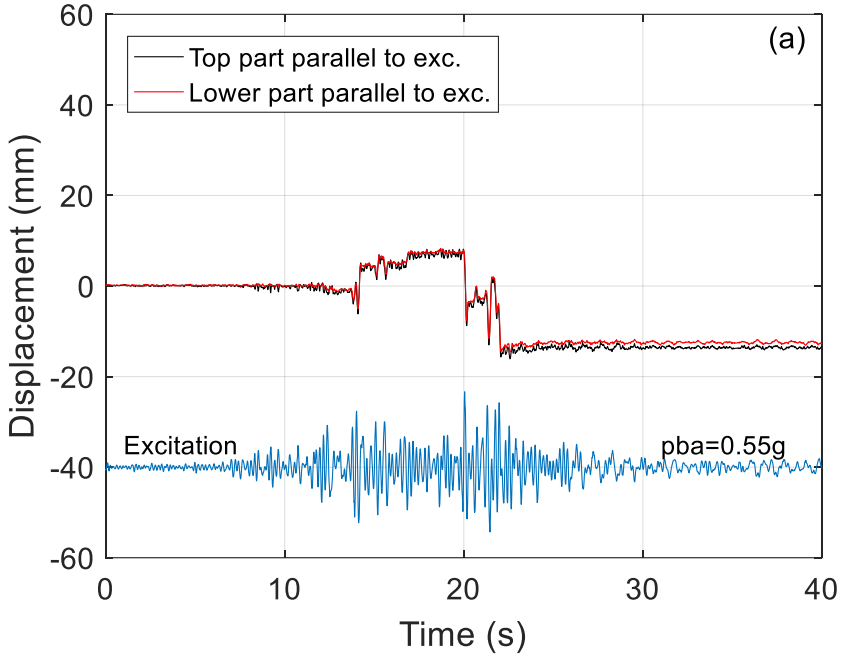

Figure 22. *Cont.*

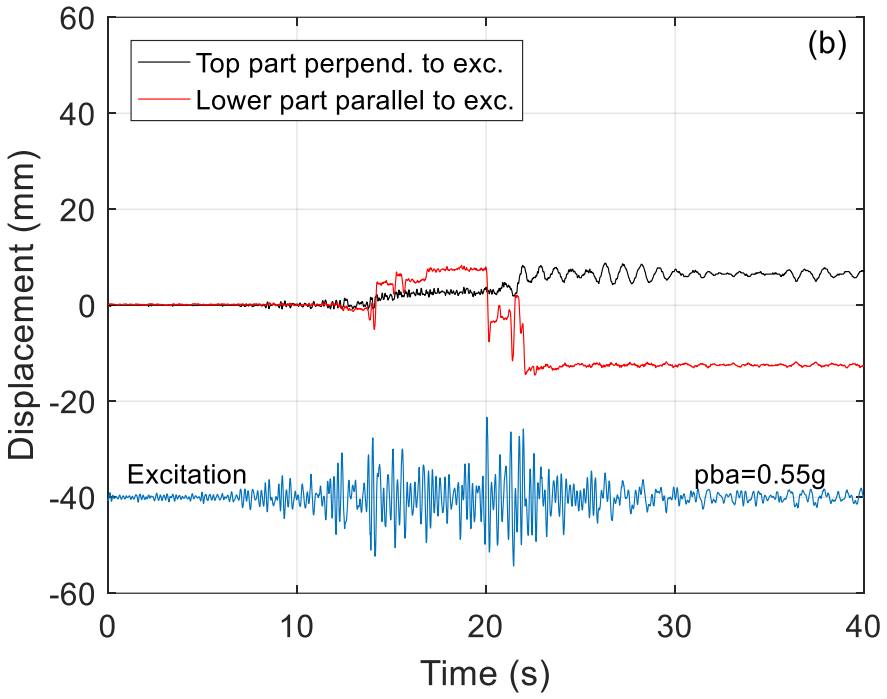

Figure 22. Response displacement of the krater for peak base acceleration 0.55 g: (**a**) top and lower part parallel to the direction of excitation; (**b**) lower part parallel and top part perpendicular to the direction of excitation (small coefficient of friction).

The increase in the coefficient of friction led to rocking when the peak acceleration was close to 0.35 g. The rocking motion was parallel to the direction of excitation and was accompanied by rotation when it was intense (Figure 23). Figure 24 shows the dynamic behavior of the vessel for the higher coefficient of friction. The sharp increase in the motion perpendicular to the direction of the excitation was due to the large motion and rotation of the vessel, which occasionally caused the laser transducer to lose contact with the vessel. This can happen when the excitation level is close to the one that causes the object to overturn. The increase in the friction level significantly affected the behavior of the vessel, leading to overturning at a peak base velocity of 0.28 m/s.

Figure 23. Photographs showing the seismic response of the krater (large coefficient of friction).

Figure 25 depicts the relative displacement of the vessel for a peak acceleration of 0.45 g. The motion of the object included intense rocking and rotation, which caused the laser measuring the motion perpendicular to the direction of excitation to lose contact with it. This can be observed in Figure 25b at the 22 s of the excitation.

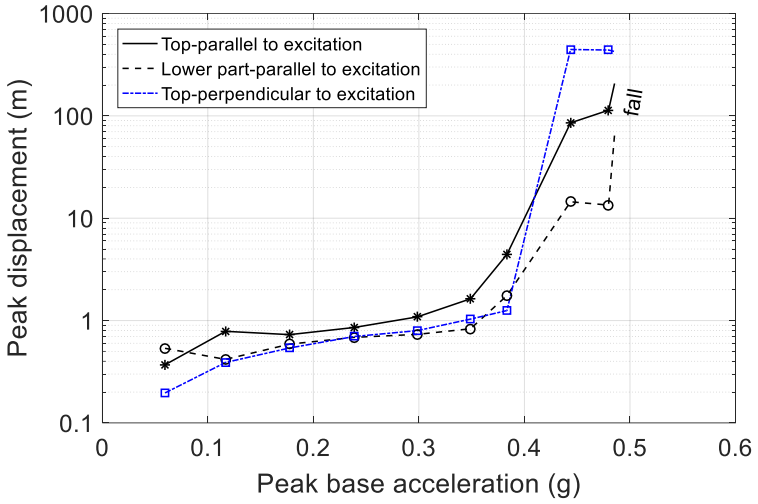

Figure 24. Peak displacement of the krater under different intensity levels of the earthquake excitation (large coefficient of friction).

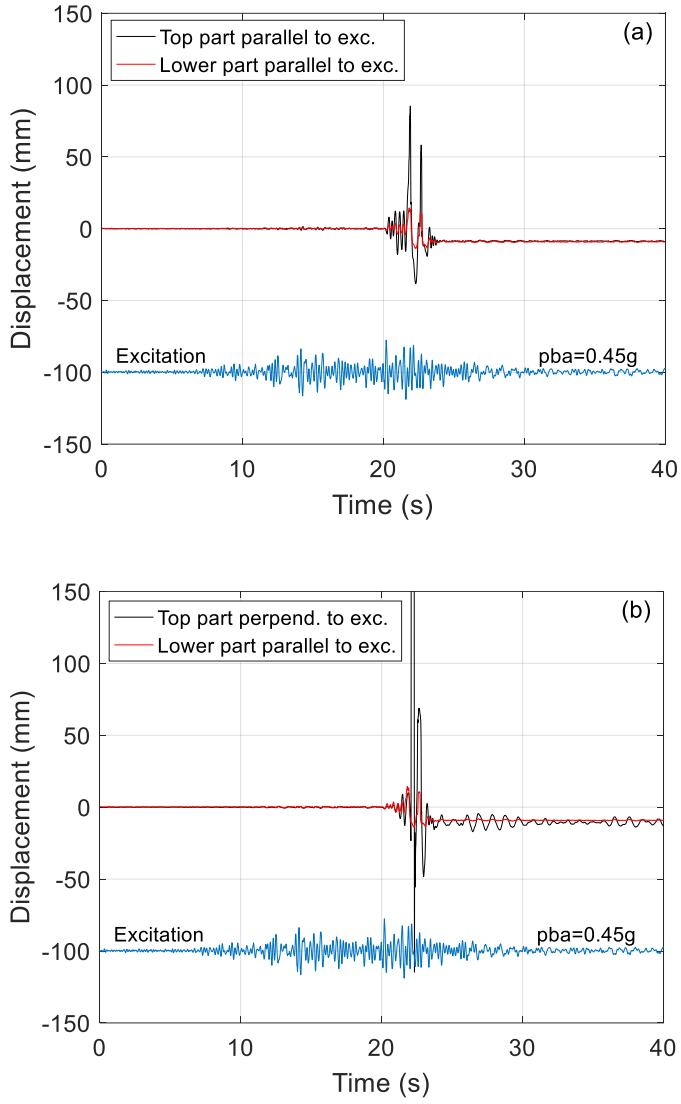

Figure 25. Response displacement of the krater for peak base acceleration 0.45 g: (**a**) top and lower parts parallel to the direction of excitation; (**b**) lower part parallel and top part perpendicular to the direction of excitation (large coefficient of friction).

4. Discussion

According to Augusti et al. [11], the horizontal velocity for overturning slender parallelepipedal objects satisfies the following expression:

$$v > 10\frac{2b}{\sqrt{2h}} \tag{1}$$

where b corresponds to half the diameter of the bottom of the vessel in cm, and h is the distance of the center of gravity of the vessel from its plane of support in cm.

According to Equation (1) and the characteristics of the vessels used in the experiments, overturning should occur at peak velocities greater than 0.12 m/s for the large and small lekythos and 0.19 m/s for the amphora and the krater. In the conducted experiments for all vessels overturning occurred at peak velocity of excitation in accordance to Equation (1). The overturning velocities observed from the conducted experiments were large lekythos 0.14 m/s, small lekythos 0.22 m/s (small coefficient of friction) and 0.14 m/s (large coefficient of friction), amphora 0.23–0.25 m/s, and krater 0.28 m/s (large coefficient of friction).

The coefficient of friction plays an important role in the seismic behavior of the vessels. A high coefficient of friction may prevent the vessel from moving. However, at high levels of excitation, depending on the geometry of the vessel, sliding or rocking can take place according to the following equations.

According to theory [11], sliding can take place if

$$|a_g| < \frac{b}{h}g \text{ and } |a_g| > \mu g \tag{2}$$

while a necessary condition for rocking is

$$|a_g| > \frac{b}{h}g \tag{3}$$

where a_g is the peak base acceleration, and μ is the coefficient of friction between the object and the plane of support.

In the conducted experiments, it was observed that the high coefficient of friction delayed the beginning of motion. When motion was initiated due to high excitation levels, it primarily involved rocking confined to a vertical plane parallel to the direction of the excitation, minimizing sliding or rotation of the vessels until overturning occurred at high excitation levels.

Sliding was observed mostly for the small coefficient of friction and for the small lekythos and the krater. Figures 10 and 21 show that at the large levels of excitation, sliding kept occurring, exceeding the first limit of Equation (2). Peak base acceleration higher than $(b/h)g$ occurred in one or two instances, followed by much lower values of acceleration, which did not suffice to invoke rocking.

Rocking occurred several times at values of peak base acceleration lower than $(b/h)g$, particularly for the large coefficient of friction, which plays an important role. The seismic behavior of objects is also influenced by the eccentricity of their center of mass [22,29] and the imperfections of their base.

It is noteworthy that (i) the difference in behavior between the small lekythos and amphora with close values of b/h, and (ii) the similarity in behavior between the small lekythos and the krater, which had a large difference in b/h but almost equal (small) height and distance of their center of gravity from their base of support. The overall geometry and existing irregularities play an important role in the dynamic behavior of the objects.

In future research, the effect of the frequency content of an excitation signal on the seismic response of the vessels will be explored using harmonic excitation, allowing the study of each frequency's impact separately. In addition, ways to minimize the motion of monumental objects and increase their seismic safety without altering their appearance

need to be studied. There is a lot of research in the area of civil engineering, where non-conventional techniques have been used to control seismic vibrations of structures [26,30]. Base isolation and dampers have already been used for the reduction in the response of large art objects [13,27]. All existing techniques can be studied and compared to identify the most appropriate method for protecting these fragile objects, considering that the materials of several have deteriorated and weakened.

5. Conclusions

The dynamic behavior of replicas of ancient vessels was examined. These replicas included two lekythos with different sizes: one amphora and one krater. The geometric characteristics, the level of excitation and the coefficient of friction at the interface of the vessel and its base of support are important parameters that influence the dynamic behavior of the vessels. The results of this study are summarized in the following paragraphs.

The large lekythos, when the coefficient of friction was small, at low levels of excitation, exhibited slight motion of the top part. At higher levels of excitation, its dynamic response included rocking and rotation around its vertical axis. Increasing the coefficient of friction led to rocking parallel to the direction of excitation, even at lower excitation levels, while reducing the out-of-plane motion. However, this did not affect the level of excitation at which overturning occurred.

The dynamic response of the small lekythos was different than the large one. When the coefficient of friction was small, its primary response was sliding parallel to the direction of excitation. Higher excitation levels, compared to the large lekythos, were required for the small lekythos to overturn. Increasing the coefficient of friction significantly affected the dynamic response of small lekythos. Sliding was minimized, visible rocking started from low levels of excitation, and overturning occurred at nearly half the base acceleration level required in the low friction case.

The main dynamic response of the amphora, when the coefficient of friction and the level of excitation were low, was rocking. The increase in the excitation level intensified rocking while initiating rotation about its vertical axis. The large coefficient of friction minimized rotation but played a less significant role than in the previous cases.

The krater had similar behavior with the small lekythos. For the small coefficient of friction, sliding parallel to the direction of excitation was the main motion. The increase in the coefficient of friction influenced considerably the behavior of the krater, producing rocking parallel to the direction of excitation, which was accompanied by rotation when the excitation was intense.

Concluding, the coefficient of friction between the interface of the vessel and its base of support plays an important role. A high coefficient of friction reduces sliding and facilitates rocking at lower levels of excitation than expected, increasing the probability of overturning.

The overall geometry of the vessel and existing irregularities also influence its dynamic behavior.

The peak base acceleration required to invoke rocking and overturning must be applied to the object for a period of time to generate the necessary conditions. Overturning will not always occur at the same level of excitation. The vessel at high levels of excitation may rock and rotate, being close to falling, but, at the last moment, may find its balance, avoiding falling.

Funding: This research received no external funding.

Institutional Review Board Statement: Not applicable.

Informed Consent Statement: Not applicable.

Data Availability Statement: The original data presented in the study are available in Zenodo at [DOI: 10.5281/zenodo.12679347].

Acknowledgments: The participation of Vassiliki Malliari in preliminary experiments was greatly appreciated.

Conflicts of Interest: The author declares no conflict of interest.

References

1. Spyrakos, C.C.; Maniatakis, C.A.; Taflampas, I.M. Assessment of seismic risk for museum artifacts. In Proceedings of the 14th World Conference on Earthquake Engineering, Beijing, China, 12–17 October 2008.
2. Spyrakos, C.C.; Maniatakis, C.A.; Taflampas, I.M. Application of predictive models to assess failure of museum artifacts under seismic loads. *J. Cult. Heritage* **2017**, *23*, 11–21. [CrossRef]
3. Venanzi, I.; Ierimonti, L.; Materazzi, A.L. Active control of art objects subjected to seismic excitation. *Procedia Eng.* **2017**, *199*, 1816–1821. [CrossRef]
4. Agbabian, M.S.; Masri, S.F.; Nigbor, R.L.; Ginell, W.S. Seismic Damage Mitigation Concepts for Art Objects in Museums. In Proceedings of the 9th World Conference on Earthquake Engineering, Tokyo-Kyoto, Japan, 2–9 August 1988; Volume VII.
5. Erdik, M.; Durukal, E.; Ertürk, N.; Sungay, B. Earthquake risk mitigation in Istanbul museums. *Nat. Hazards* **2010**, *53*, 97–108. [CrossRef]
6. Berto, L.; Favaretto, T.; Saetta, A.; Antonelli, F.; Lazzarini, L. Assessment of seismic vulnerability of art objects: The "Galleria dei Prigioni" sculptures at the Accademia Gallery in Florence. *J. Cult. Heritage* **2012**, *13*, 7–21. [CrossRef]
7. Podany, J. An overview of seismic damage mitigation for museums. In Proceedings of the International Symposium on Advances of Protection Devices for Museum Exhibits 2015, Beijing and Shangai, China, 13–17 April 2015.
8. Viti, S.; Tanganelli, M. Resimus: A Research Project on the Seismic Vulnerability of Museums' Collections. In Proceedings of the 7th ECCOMAS International Conference on Computational Methods in Structural Dynamics and Earthquake Engineering, COMPDYN 2019, Crete, Greece, 24–26 June 2019. [CrossRef]
9. Liu, P.; Li, Z.-H.; Yang, W.-G. Seismic fragility analysis of sliding artifacts in nonlinear artifact-showcase-museum systems. *Struct. Eng. Mech.* **2021**, *78*, 333–350. [CrossRef]
10. Housner, G.W. The behavior of inverted pendulum structures during earthquakes. *Bull. Seism. Soc. Am.* **1963**, *53*, 403–417. [CrossRef]
11. Augusti, G.; Ciampoli, M.; Airoldi, L. Mitigation of seismic risk for museum contents: An introductory investigation. In Proceedings of the Earthquake Engineering, Tenth World Conference, Madrid, Spain, 19–24 July 1992; Balkerma: Rotterdam, The Netherlands, 1992; Volume 9, pp. 5995–6000.
12. Lipscombe, P.R.; Pellegrino, S. Free Rocking of Prismatic Blocks. *J. Eng. Mech.* **1993**, *119*, 1387–1410. [CrossRef]
13. Calio, I.; Marletta, M. On the mitigation of the seismic risk of art objects: Case studies. In Proceedings of the 13th World Conference on Earthquake Engineering, Vancouver, BC, Canada, 1–6 August 2004.
14. Vassiliou, M.F.; Makris, N. Analysis of the rocking response of rigid blocks standing free on a seismically isolated base. *Earthq. Eng. Struct. Dyn.* **2011**, *41*, 177–196. [CrossRef]
15. Makris, N. A half-century of rocking isolation. *Earthquakes Struct.* **2014**, *7*, 1187–1221. [CrossRef]
16. Ther, T.; Kollár, L.P. Refinement of Housner's model on rocking blocks. *Bull. Earthq. Eng.* **2016**, *15*, 2305–2319. [CrossRef]
17. Manzo, N.R.; Vassiliou, M.F. Displacement-based analysis and design of rocking structures. *Earthq. Eng. Struct. Dyn.* **2019**, *48*, 1613–1629. [CrossRef]
18. Liu, H.; Huang, Y.; Liu, X. Seismic Overturning Fragility Analysis for Rigid Blocks Subjected to Floor Motions. *Sustainability* **2023**, *15*, 4945. [CrossRef]
19. Scalia, A.; Sumbatyan, M. Slide rotation of rigid bodies subjected to a horizontal ground motion. *Earthq. Eng. Struct. Dyn.* **1996**, *25*, 113901149. [CrossRef]
20. Shenton, H.W., III. Criteria for Initiation of Slide, Rock, and Slide-Rock Rigid-Body Modes. *J. Eng. Mech.* **1996**, *122*, 690–693. [CrossRef]
21. Diamantopoulos, S.; Fragiadakis, M. Seismic response and fragility assessment of freestanding objects with random geometry. *Soil Dyn. Earthq. Eng.* **2024**, *181*, 108649. [CrossRef]
22. Wittich, C.E.; Hutchinson, T.C. Shake table tests of unattached, asymmetric, dual-body systems. *Earthq. Eng. Struct. Dyn.* **2017**, *44*, 2425–2443. [CrossRef]
23. Liu, P.; Zhang, Y.; Chen, H.; Yang, W. Experimental study on rocking blocks subjected to bidirectional ground and floor motions via shaking table tests. *Earthq. Eng. Struct. Dyn.* **2023**, *52*, 3171–3192. [CrossRef]
24. Huang, B.; Günay, S.; Lu, W. Seismic Assessment of Freestanding Ceramic Vase with Shaking Table Testing and Performance-Based Earthquake Engineering. *J. Earthq. Eng.* **2021**, *26*, 7956–7978. [CrossRef]
25. Prota, A.; Zito, M.; D'Angela, D.; Toscano, G.; Ceraldi, C.; Fiorillo, A.; Magliulo, G. Dynamic Properties and Seismic Response of a Museum Display Case with an Art Object. In *Seismic Isolation, Energy Dissipation and Active Vibration Control of Structures. WCSI 2022*; Cimellaro, G.P., Ed.; Lecture Notes in Civil Engineering; Springer: Cham, Switzerland, 2023; Volume 309. [CrossRef]
26. Papalou, A.; Strepelias, E.; Roubien, D.; Bousias, S.; Triantafillou, T. Seismic protection of monuments using particle dampers in multi-drum columns. *Soil Dyn. Earthq. Eng.* **2015**, *77*, 360–368. [CrossRef]

27. Siami, A.; Cigada, A.; Karimi, H.R.; Zappa, E. Vibration Protection of a Famous Statue against Ambient and Earthquake Excitation Using A Tuned Inerter–Damper. *Machines* **2017**, *5*, 33. [CrossRef]
28. Monaco, M.; Guadagnuolo, M.; Gesualdo, A. The role of friction in the seismic risk mitigation of freestanding art objects. *Nat. Hazards* **2014**, *73*, 389–402. [CrossRef]
29. Al Abadi, H.; Paton-Cole, V.; Gad, E.; Lam, N.; Patel, V. Rocking Behavior of Irregular Free-Standing Objects Subjected to Earthquake Motion. *J. Earthq. Eng.* **2019**, *23*, 793–809. [CrossRef]
30. Dong, Y.-R.; Xu, Z.-D.; Li, Q.-Q.; He, Z.-H.; Yan, X.; Cheng, Y. Tests and Micro–Macro Cross-Scale Model of High-Performance Acrylate Viscoelastic Dampers Used in Structural Resistance. *J. Struct. Eng.* **2023**, *149*. [CrossRef]